*Rev. Roum. Sci. Techn.– Électrotechn. et Énerg.*
Vol. **66**, *2*, pp. 131–136, Bucarest, 2021

**Thermotechnique et thermoénergétique**

# A DIRECT ADAPTIVE SLIDING MODE HIGH VOLTAGE GAIN PEAK POWER TRACKER FOR THERMOELECTRIC APPLICATIONS

ABDELHAKIM BELKAID [1], ILHAMI COLAK [2], KORHAN KAYISLI [2]

**Key words: Thermoelectric applications, Maximum power point tracking (MPPT), Direct adaptive sliding mode, Single-ended primary-inductor converter (SEPIC), High voltage gain converter.**

**Today, thermoelectric generators (TEG) are of great interest since their prices are falling and more areas of applications have appeared. In order to increase the TEG's low voltage and to enhance performance of the thermoelectric power conversion system, this paper presents a direct adaptive sliding mode MPPT based on incremental conductance (INC) principle applied to a modified high voltage gain SEPIC converter. Mathematical modeling and computer simulations for the considered system are carried out. A comparison is made between the proposed method, the basic sliding mode (SM) and the Perturb and Observe (P&O) algorithm. The proposed tracker has been implemented to ensure that the TEG works at its maximum power regardless of the load it feeds and the temperature gradient between its two sides. The results of this study showed that the TEG's voltage can be boosted from two to twenty times, an energy transfer efficiency over than 99% and an aptitude to track the maximum power point (MPP) at diverse working conditions perfectly with high performance including low convergence time and less oscillations.**

## 1. INTRODUCTION

Every day, a significant amount of thermal power is lost especially in the industrial and transport sectors. This lost energy can be valorized in order to increase the energy yields of the systems. To recover some of the unused heat, a TEG [1–2] can be used. TEGs have significant assets at low power like long service life, small dimension, light heaviness, silent, independent of climate, no greenhouse gas emissions, low cost of maintenance and non-exhaustible source. However, TEG efficiency is usually less than 10 % [2].

A TEG like a photovoltaic (PV) generator admits a unique point that allows its optimal operation. So, a control algorithm is needed to pursuit the MPP of the apparatus. A lot of MPPT techniques concentrated on PV applications were described in several references like P&O [3] and INC [4]. The neural network [5] and the fuzzy logic control [6] have also been used with success in PV systems. These MPPTs are capable to track the maximum power accurately in stable conditions. But there must be a compromise between tracking speed and accuracy when choosing the step size [7].

We now come to the SM technique, which has many advantages; it is accurate, fast, robust and uncomplicated. It is often employed in variable structure systems as static converters [8]. Recently, the SM method is applied to PV applications. In [9], the MPPT control consists of P&O algorithm in cascade with a PI regulator. The latter has drawbacks such as: slow transient response, big overshoot and important steady state oscillations. To overcome these problems, some researches as in [10 –11] use a SM regulator instead of the PI regulator to improve voltage regulation and thus improve tracking of maximum PV power. These methods make the PV system more complex. In order to reduce this complexity, our document proposes a direct sliding mode method without calling on other MPPT methods. The proposed method aims to improve the static and dynamic performance of the TEG. It consists of a direct adaptive step size SM-MPPT using the INC principle. The INC principle is employed to determine the equivalent control and the variable step size is employed in the switching control law. A big step size is utilized when the working point is far from the peak power to increase the tracking speed, but a small step size is utilized when the operating point is in close proximity to the MPP in order to decrease the surrounding oscillations. To distinguish between these two situations, the absolute value of the slope of the power-voltage curve ($\left|\mathrm{d}P/\mathrm{d}V\right|$) is compared to a small selected value $\varepsilon$. If $\left|\mathrm{d}P/\mathrm{d}V\right|<\varepsilon$, the new step size is similar to the step size of the basic SM ($\text{step}=k_{SM}$), but if $\left|\mathrm{d}P/\mathrm{d}V\right|>\varepsilon$, the new step size takes a multiple of the fixed step size ($\text{step}=k_{SM}$), where $a$ is a large positive number. In accordance with the modifications mentioned above, the convergence time and the fluctuations around the peak power will be reduced. Thus, the performance of the proposed control system will be enhanced under temperature gradient variation in comparison to P&O and conventional SM.

Because the TEG delivers a low-voltage direct current, the second contribution of this work is the use of a SEPIC-type voltage booster converter with a high transformation ratio ($V_0/V=2/(1-d)$).

The rest of the document is planned as follows; Section 2 offers a mathematical model to the TEG module while the detailed analysis of the operating principle of the SEPIC converter with high voltage gain is given in section 3. The basics of the proposed adaptive SM-MPPT method are reported in part 4. The simulation results with some comparisons are presented in Part 5. The paper ends with some conclusions and perspectives.

## 2. THERMOELECTRIC MODULE MODEL

The HZ-20 thermoelectric module [11], by HiZ manufacturer, which uses bismuth telluride $Bi_2Te_3$, is used. When applying a temperature gradient ($\Delta T=T_H-T_C$), where $T_H$ is the hot plate and $T_C$ is the cold plate, between the two surfaces, a voltage is generated as shown in Fig. 1a.

[1] Electrical Engineering Department, University of Bejaia, Algeria, e-mail: belkaid08@yahoo.fr
[2] Engineering and Architecture Faculty of Nisantasi University, Istanbul, Turkey

The thermal power absorbed by the hot face $Q_H$ and the thermal power liberated by the cold face $Q_C$ are as in [12]:

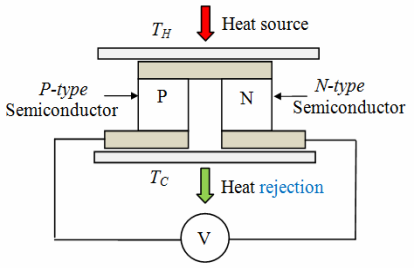


Fig. 1 – a) Elementary thermoelectric generator

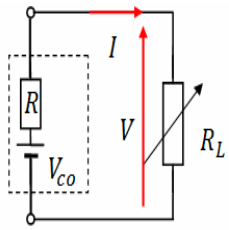


Fig. 1 – b) Electrical model of a TEG

$$Q_H = \alpha I T_H + k(\Delta T) - 0.5RI^2 \quad (1)$$

$$Q_C = \alpha I T_C + k(\Delta T) + 0.5RI^2 . \quad (2)$$

where $I$ and $V$ are respectively the output current and the output voltage, $k$ is the thermal conductance, $\alpha$ represent the Seebeck coefficient and $R$ is the internal electrical resistance.

The power $P$ produced by a TEG can be calculated as:

$$P = V \cdot I = Q_H - Q_C = \alpha I(\Delta T) - RI^2 . \quad (3)$$

Thus, the voltage can be expressed as:

$$V = \alpha(\Delta T) - RI . \quad (4)$$

When, there is no load connected to the TEG, the voltage takes its high value, the open circuit voltage:

$$V_{co} = \alpha(\Delta T) . \quad (5)$$

From (4) and (5), we can get:

$$V = V_{co} - RI . \quad (6)$$

According to (6), a model of a TEG can be obtained as the open circuit voltage source connected in serial manner to its internal resistor as shown in Fig. 1b. The characteristics obtained by simulation at various temperature gradients for the selected TEG are shown in Fig. 2. The power vs. voltage curves that have a parabolic form is depicted in Fig. 2a. For each temperature gradient, the peak power point designated by black dot is located at the operating voltage corresponding to the half of the open circuit voltage. Fig. 2b confirms the linearity of the current vs. voltage curves.

## 3. THE HIGH VOLTAGE GAIN SEPIC CONVERTER

The selection of a static converter depends on the voltage existing at its entry and on the preferred voltage at its output. The SEPIC converter in its traditional structure deserves more interest because of its high performance, low ripples, non-inversion of the exit voltage, and it can augment or diminish the voltage level. Because of the low voltage direct current of the TEG, it is preferable to use high gain dc/dc converters. Several authors have modified conventional dc/dc converters to lift the input voltage. Among them, Ozsoy *et al.* have proposed modified Cuk in [13] and modified SEPIC in [14]. Also, Babaei *et al.* have proposed high step-up nonisolated converter by combining a double-boost and SEPIC structure in [15]. For the reasons mentioned above, we prefer that the high voltage rate SEPIC converter be inserted between the low voltage TEG source and the load to adjust the voltage levels and track the peak power. From the conventional to the modified SEPIC, the voltage gain can be increased from $d/(1-d)$ to $2/(1-d)$ where $d$ is the duty cycle of the SEPIC. The new converter can be formed from the old one by adding an inductor, 2 diodes and 3 capacitors as shown in Fig. 3.

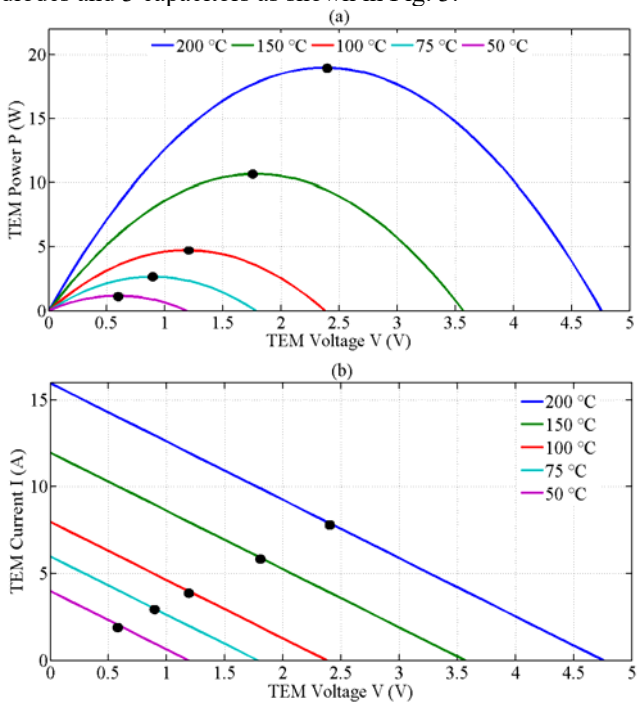


Fig. 2 – HZ-20 module characteristics: a) *P-V* curves; b) *I-V* curves.

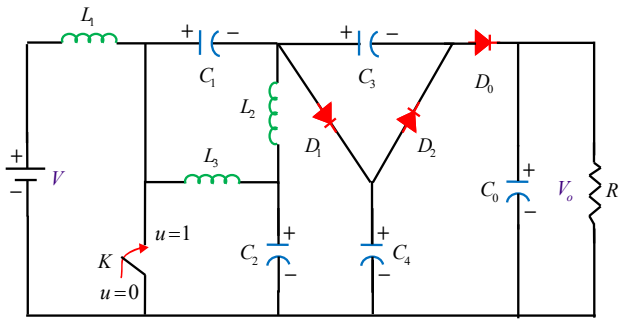


Fig. 3 – Modified SEPIC structure.

In steady state, the average voltage of an inductor is set to zero and therefore if the Kirchhoff law is applied to the loop which contains $C_1$ , $L_2$ and $L_3$, we obtain that the voltage across the capacitor is zero.

$$V_{C_1} = 0 . \quad (7)$$

When the switch $k$ is in the ON position, the diodes $D_1$ and $D_0$ are off, the diode $D_2$ is activated, and then the equations of the static converter can be depicted as follows:

$$V_{L_1} = V \quad (8)$$

$$V_{C_1} + V_{C_3} + V_{C4} = V_{C_3} + V_{C_4} = 0 . \quad (9)$$

When the semiconductor $k$ is in the OFF position, the diodes $D_1$ and $D_0$ are on, the diode $D_2$ is deactivated, and then the converter equations become:

$$V_{C_1} + V_{C_4} + V_{L_1} = V_{C_4} + V_{L_1} = V \tag{10}$$

$$V_0 + V_{C_2} - V_{C_4} = 0\,. \tag{11}$$

The volt-second balanced rule can be applied for the inductance $L_1$ using equations (8) and (10):

$$d(V) + (1+d)(V - V_{C_4}) = 0 \tag{12}$$

$$V_{C_4} = \frac{1}{1-d} V\,. \tag{13}$$

Based on Eqs. (9) and (11), the average voltage across the capacitor $C_4$ can be formulized as:

$$V_{C_4} = \frac{1}{2} V_0\,. \tag{14}$$

By dividing Eqs. (14) on Eq. (13), we obtain the equation of the transformation ratio of the converter as:

$$V_0 = \frac{2}{1-d} V\,. \tag{15}$$

By using the power conservation tenet between the two sides of the converter, the gain in current can be expressed as:

$$\frac{I_0}{I} = \frac{1-d}{2}\,, \tag{16}$$

where $I_o$ is the output current.

In theory, $d$ can take values between 0 and 1, the voltage gain is therefore between 2 and + ∞. But practically $d$ is limited to between 0.1 and 0.9, which implies that the voltage gain can have values between 2.22 and 20. This means that the modified SEPIC can function as a good voltage booster but can never act as a step-down voltage, unlike the traditional converter.

## 4. TEG MODULE MPPTS

### 4.1. THE PERTURBATION AND OBSERVATION METHOD

The P&O scheme is largely utilized to maximise the PV power generation and recently is also employed for TEG applications [15, 16]. It is the most implemented in practice due to its simple structure. It engages a disturbance at regular intervals in the voltage of the renewable source or in the duty ratio of the static converter and after it compares the current power to the previous one. The P&O algorithm is capable to track the maximum power harvested but it suffers from two important problems; the first consists on the oscillations in the region of the true MPP in fixed conditions, the second is the low performance in dynamic when the entries vary abruptly.

### 4.2. THE CONVENTIONAL SLIDING MODE METHOD

The basic SM consists of two key actions; the selection of a sliding surface $S$ and the designing of a switching law $u$ which can attract the positions of the entire system in a wanted behaviour $S = 0$ [7].

According to the curves exposed in Fig.2, the module works at its MPP, when $dP/dV = 0$. Thus, we can choose $S = dP/dV$.

The control law $u$ can be expressed as:

$$u = u_n + u_{eq}\,, \tag{17}$$

$u_n$, the switching control, is equal typically to:

$$u_n = -k_{SM}\,\mathrm{sign}(S)\,, \tag{18}$$

where $k_{SM}$ is a positive constant, aiming to make sure the attractiveness of every functioning point into the sliding surface and assure the convergence situation

### 4.3. THE Adaptive SM-MPPT Method

The principle of the modified method is illustrated in Fig. 4. Two zones for the operating point are considered, they have been delimited by an epsilon parameter ε known as an allowed error. The first region is located near the MPP, but the second is situated far (left or right) from the MPP. The proposed tracker uses variable step size as following:

$$u = u_{eq} - \mathrm{step}\frac{dP}{dV} \tag{19}$$

$$\begin{cases} \mathrm{step} = k_{SM} \rightarrow \text{if } |dP/dV| < \varepsilon \\ \mathrm{step} = \alpha k_{SM} \rightarrow \text{if } |dP/dV| > \varepsilon \end{cases}. \tag{20}$$

It uses a large step size ( $\mathrm{step} = a \cdot k_{SM}$ ) to displace rapidly the working point located in the second zone ( $|dP/dV| > \varepsilon$ ) to the first zone ( $|dP/dV| < \varepsilon$ ) and thus the convergence speed will be increased. In order to reduce the magnitude of the neighboring undulations, the proposed algorithm uses a small step size ( $\mathrm{step} = k_{SM}$ ).

The parameter $u_{eq}$ can be determined using the equalities of the invariance condition ($S = 0$ and $\frac{dS}{dt} = 0$) [7, 8]

$$S = \frac{dP}{dV} = \frac{d(VI)}{dV} = I + V\frac{dI}{dV} \tag{21}$$

$$S = \frac{dP}{dV} \rightarrow \frac{1}{V} + \frac{dI}{dV} = G + dG = 0\,, \tag{22}$$

where $G$ is the instantaneous conductance and $dG$ is the incremental conductance.

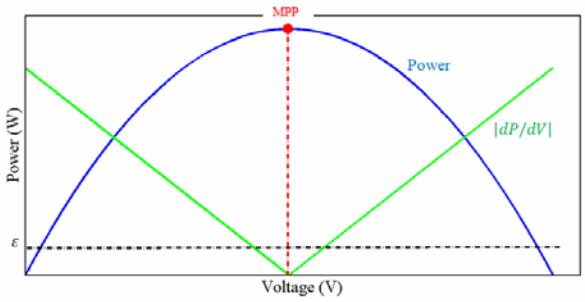


Fig. 4 – Principle of the proposed SM-MPPT.

$$\frac{dS}{dt} = 0 \rightarrow \frac{dG}{dt} + \frac{d}{dt}(dG) = 0\,, \tag{23}$$

$$\frac{dS}{dt} = 0 \rightarrow \left[\frac{dG}{dt} + \frac{d}{dt}(dG)\right] \cdot \frac{dI}{dI} = 0\,, \tag{24}$$

$$\left[\frac{\mathrm{d}G}{\mathrm{d}I}+\frac{\mathrm{d}}{\mathrm{d}I}(\mathrm{d}G)\right]\cdot\frac{\mathrm{d}I}{\mathrm{d}t}=0. \quad (25)$$

Since $G$ and d$G$ are dependent of $I$ . Eq. (25) becomes:

$$\frac{\mathrm{d}I}{\mathrm{d}t}=0\rightarrow u=u_{eq}, \quad (26)$$

$$L_1\frac{\mathrm{d}I}{\mathrm{d}t}=V\rightarrow \text{for}\rightarrow u=1\,, \quad (27)$$

$$L_1\frac{\mathrm{d}I}{\mathrm{d}t}=V-V_o-V_{C_1}-V_{C_3}\rightarrow \text{for}\rightarrow u=0. \quad (28)$$

From (9) and (11), we get:

$$V_{C_3}=-V_0/2. \quad (29)$$

By replacing (7) and (29) in Eq. (28), we obtain:

$$L_1\frac{\mathrm{d}I}{\mathrm{d}t}=V-\frac{V_0}{2}\rightarrow \text{for}\rightarrow u=0. \quad (30)$$

From Eq. (27) and (30), we get:

$$L_1\frac{\mathrm{d}I}{\mathrm{d}t}=V+(u-1)\frac{V_0}{2}. \quad (31)$$

From (26) and (31), we get:

$$V+(u_{eq}-1)\frac{V_0}{2}=0\Rightarrow u_{eq}=1-\frac{2V}{V_0}. \quad (32)$$

Finally, $u$ is obtained as:

$$u=1-\frac{2V}{V_0}-\text{step}\cdot\frac{\mathrm{d}P}{\mathrm{d}V}. \quad (33)$$

In accordance with the changes made to the original algorithm, the response time and the fluctuations around the MPP will be decreased. Consequently, the power transfer performance achieved by the proposed control system will be better comparing to P&O and original SM.

## 5. SIMULATION RESULTS

Figure 5 provides the scheme of the TEG system. The different parameters used in simulation will be given in Table 1.

*Table 1*
Modified SEPIC converter parameters

| Parameter | Label | Value |
|---|---|---|
| Frequency | $f$ | 50 kHz |
| Inductance | $L_1$ | 5 mH |
| Inductances | $L_{2,3}$ | 0.1 mH |
| Capacitors | $C_{1,2,3,4}$ | 5 µF |
| Capacitor | $C_o$ | 10 µF |
| Capacitor | $C_{teg}$ | 1 µF |
| Resistive load | $R$ | 25 Ω |

### 5.1. BASIC *VS.* PROPOSED SLIDING MODE MPPT

To make obvious the effectiveness of the proposed method, the TEG system is simulated using Matlab. A comparison between P&O, basic SM and proposed SM, is carried out. The cold side temperature is kept constant at 30 °C but the hot side temperature is changed in order to have the temperature gradient like a square signal between 100 and 200 °C.

Figure 6 demonstrates that the actual power harvested using the proposed MPPT is close to the ideal MPP and that the conversion efficiency is close to unity. Figure 6a compares the power generated by the three MPPTs with the true peak power. Three enlarged images are added to better see the difference. The start-up zoom explains that the time required for the proposed method before reaching the permanent regime is less than that required by the other two MPPTs. The middle zoom indicates that the MPP obtained with the proposed SM-MPPT is ripple-free and close to the true MPP. The third zoom aims to show the effectiveness of the different methods after a sudden drop in the temperature. A comparison between the power transfer efficiency behaviors obtained by these techniques is given in Fig. 6b.

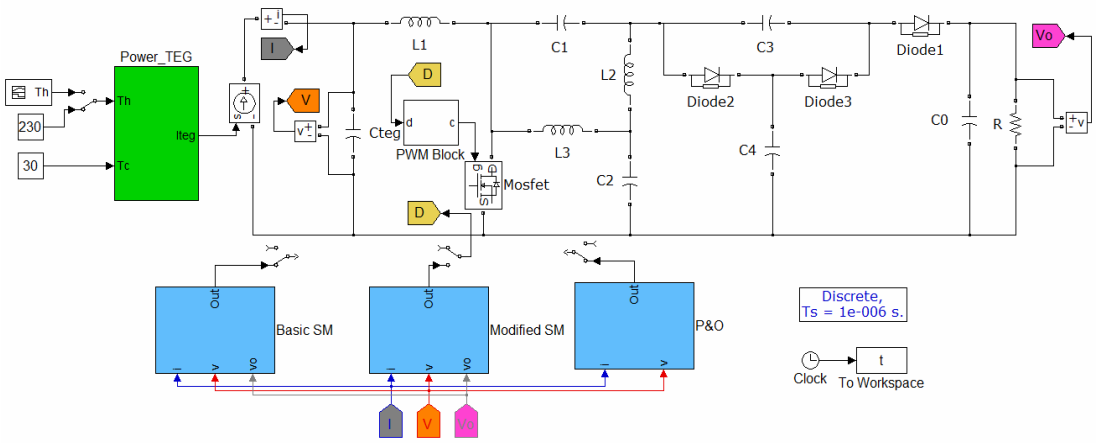


Fig. 5 – The high voltage gain SEPIC peak power tracker for TEG.

The efficiency of the power transfer $T_{eff}$ is calculated by the ratio of the maximum power $P_{MPPT}$ obtained using a given MPPT method to the true maximum power $P_{max}$.

$$T_{eff} = \frac{\int_0^t P_{MPPT} \cdot dt}{\int_0^t P_{max} \cdot dt} 100\%. \quad (34)$$

For a good comparison of the performances of the studied techniques, the mean value of their yields is calculated. The best average efficiency is obtained by the proposed SM, its value is equal to: 98.77 %, followed by 98.45 % for P&O and then by 98.36 % for the conventional SM. In addition, it can be seen that the proposed technique has an instantaneous tracking efficiency greater than 99 % at any time, except for the moment of change where the curve has deep descents.

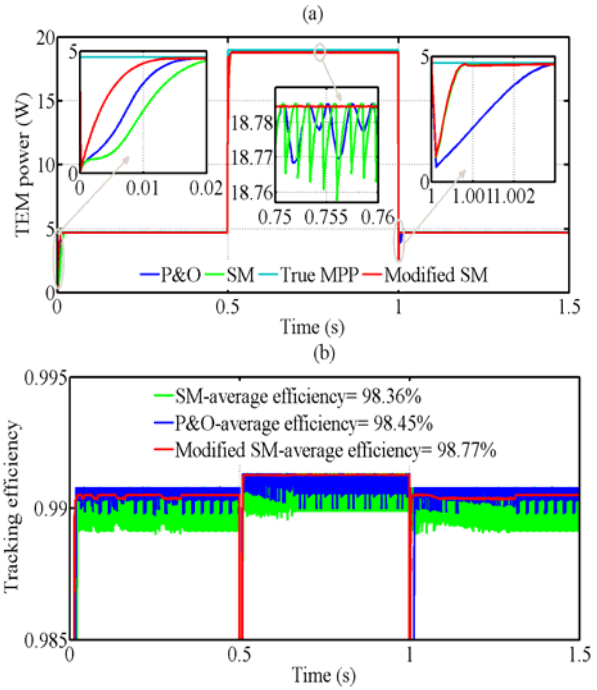


Fig. 6 – Control performance: a) power curves; b) average efficiency.

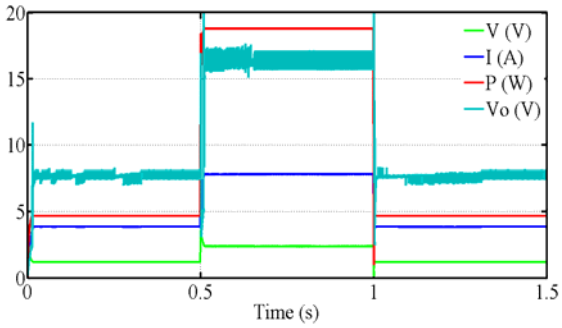


Fig. 7 – Results simulated during a variable temperature gradient test: the maximum power, voltage at MPP, current at MPP, and the load voltage.

The results continue with Fig. 7, which shows the waveforms of current at MPP, $I$(A), voltage at MPP, $V$ (V), maximum power, $P$(W), and the output voltage corresponding, $V_0$ (V), for the proposed technique under the temperature gradient profile. The latest results verify that all waveforms perfectly follow the test profile and also confirm that the static converter used in this work is of the voltage booster type.

## 5.2. CONVENTIONAL *VS.* MODIFIED SEPIC CONVERTER

Now, the system performances obtained with the proposed SM algorithm applied to the modified topology of the SEPIC converter are compared with those obtained with the same command applied on the classical SEPIC topology. The corresponding results are depicted in Fig. 8.

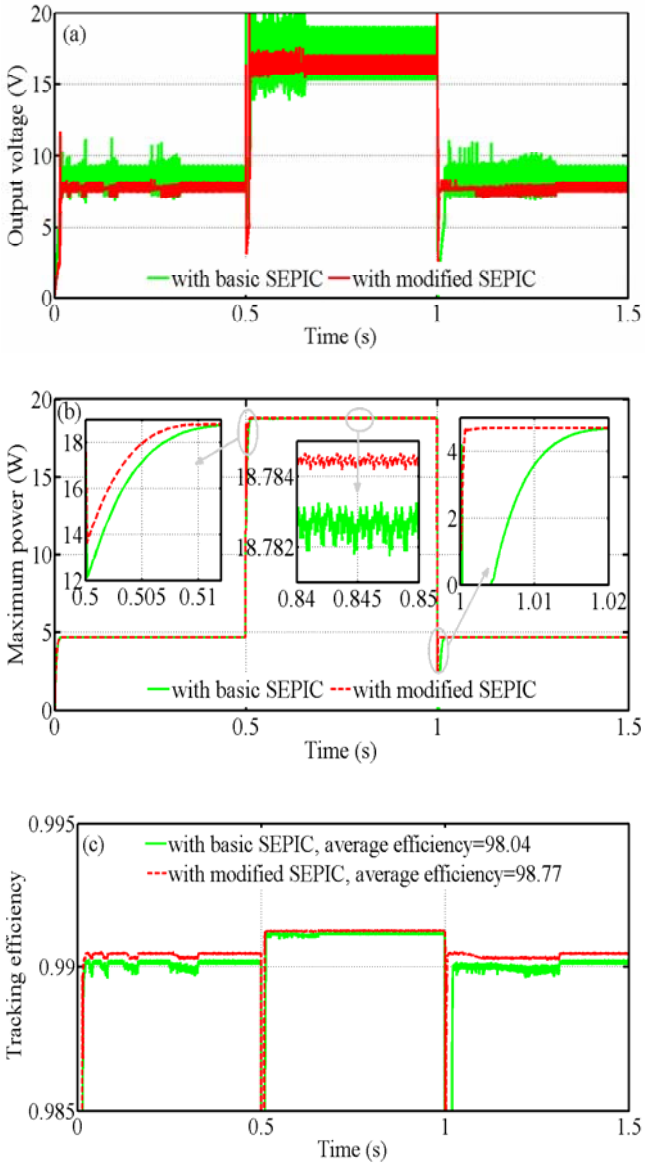


Fig. 8 – Comparison basic *vs.* modified SEPIC: a) output voltage; b) maximum power; c) average efficiency.

Figure 8 a shows the evolution of the voltage across the load for the two structures of the SEPIC converter. The modified converter allows less oscillation. Figure 8b explains the evolution of maximum power by zooming in three different places. Left zoom and right zoom indicate transients when the change profile follows a step up or down, respectively. We can see that the temporal response is improved if we use the modified topology. The central zoom shows the comparison between the MPP harvested in steady state with the two converters.

With the proposed converter, one can gain about 2 mW in every second. The efficiency of the power transfer performed using the adaptive SM-MPPT for both converters is compared as shown in Fig. 8c. If the basic SEPIC is replaced by the modified one, the yield can be increased from 98.04 to 98.77 %.

### 5.3. VARIABLE LOAD TEST

In this part, the robustness against the load disturbances of the proposed system is verified. Temperature gradient was maintained at 200 °C during load change tests. According to the HZ-20 characteristics shown in Fig. 2, the theoretical quantities of the TEG device at this point are $P = 19$ W, $V = 2.4$ V, and $I = 7.9$ A. The load is changed according to a descending staircase from 40 Ω to 20 Ω and then to 13 Ω. It can be seen from the corresponding results shown in Fig. 9 that the quantities obtained are not affected by the conditions of the charge variation and are approximately equal to the theoretical quantities. The only parameter that is influenced by the load change is the output voltage.

Finally, from the results obtained through the simulations, we can conclude that, with a well-designed power conditioning system counting a good DC-DC converter doted by a competent MPPT scheme, the performance of the entire system can be improved both in static and dynamic regimes.

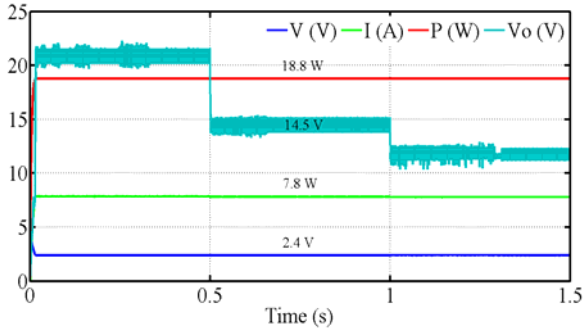


Fig. 9 – Results simulated during a variable load test: the maximum power, voltage at MPP, current at MPP, and the load voltage.

## 6. CONCLUSIONS

This document has presented a well-designed power conditioning system including a thermoelectric module, a high gain voltage step-up converter and a cost-efficient MPPT method. A modified high voltage gain SEPIC converter is used to increase the low voltage of the TEG. A direct adaptive SM maximum power-tracking scheme using the INC principle is proposed to enhance the performance of the power transfer system. Mathematical modeling, numerical simulations in the Matlab environment and optimization of the whole system are realized. The proposed control technique for the TEG peak power tracking has been tested under a square temperature difference, and compared to basic SM and P&O strategies. The results of simulation demonstrate that, the proposed MPP tracker has conversion efficiency over than 99 % and an ability to track the MPP perfectly with a high performance in both stable and active states.

*Received on December 27, 2019*

## REFERENCES

1. A. M. Morega, M. Morega, M. A. Panait, *Structural optimization of a thermoelectric generator by numerical simulation*, Rev. Roum. Sci. Techn. – Électrotechn. et Énerg., **55**, *1*, pp. 3–12 (2010).
2. D. Champier, *Thermoelectric Generators: A Review of Applications*, Energy Conversion and Management, **140**, pp. 167–181 (2017).
3. P. S. Sikder, N. Pal, K. S. Patro, *A modeling of stand-alone solar photo-voltaic system for rural electrification purposes*, Rev. Roum. Sci. Techn. – Électrotechn. et Énerg., **64**, *3*, pp. 241–246 (2019).
4. A. Belkaid, I. Colak, O. Isik, *Photovoltaic maximum power point tracking under fast varying of solar radiation*, Applied Energy, **179**, pp. 523–530 (2016).
5. H. A. Azzeddine, M. Tioursi, D. Chaouch, B. Khiari. *An offline trained artificial neural network to predict a photovoltaic panel maximum power point*, Rev. Roum. Sci. Techn.– Électrotechn. et Énerg., **61**, *3*, pp. 255–257 (2016).
6. S. P. Bihari, P. K. Sadhu, S. Das, P. Arvind, A. Gupta. *Design and implementation of a photovoltaic wind hybrid system with the assessment of fuzzy logic maximum power point technique*, Rev. Roum. Sci. Techn.– Électrotechn. et Énerg., **64**, *3*, pp. 235–240 (2019).
7. A. Belkaid, J-P. Gaubert, A. Gherbi,. *An Improved Sliding Mode Control for Maximum Power Point Tracking in Photovoltaic Systems*, Journal of Control Engineering and Applied Informatics, **18**, *1*, pp. 86–94 (2016).
8. A. Belkaid, J-P. Gaubert, A. Gherbi. *Design and Implementation of a High Performance Technique for Tracking Photovoltaic Peak Power*, IET Renewable Power Generation, **11**, *1*, 92–99 (2017).
9. M. A. Elgendy, B. Zahawi, D.J. Atkinson. *Assessment of Perturb and Observe MPPT Algorithm Implementation Techniques for PV Pumping Applications*, IEEE Transactions on Sustainable Energy, **3**,*1*, pp. 21–33 (2012).
10. M. Farhat, O. Barambones, L. Sbita, *A new maximum power point method based on a sliding mode approach for solar energy harvesting*, Appl. Energy, **185 (P2)**, pp. 1185–1198 (2017).
11. E. Bianconi, J. Calvente, R. Giral *et al. Perturb and observe MPPT algorithm with a current controller based on the sliding mode*, Int. J. Electr. Power Energy Syst., **44**, *1*, pp. 346–356 (2013).
12. J. B. Dumitru, A. M. Morega, M. Morega. *A numerical study of the heat transfer management provided by a thermoelectric sink-and-fan system*, Rev. Roum. Sci. Techn.– Électrotechn. et Énerg., **58**, *2*, pp. 205–214 (2013).
13. E. Ozsoy, S. Padmanaban, A.W. Oluwafemi, K.Vigna, T. Sutikno, *Modified (2/1-k) output gain Ćuk DC-to-DC converter circuit for renewable power applications*, IEEE 12th International Conference on Compatibility, Power Electronics and Power Engineering, Doha, Qatar, 10-12 April 2018.
14. E. Ozsoy, S. Padmanaban, V. Fedak, C. Muranda, M. Cernet, *Modified SEPIC DC-to-DC Converter 2/(1-k) Output Gain Configuration for Renewable Power Energy and High Voltage Applications,* IEEE 18th International Power Electronics and Motion Control Conference (PEMC), Budapest, Hungary, 26-30 August 2018.
15. E. Babaei, T. Jalilzadeh, M. Sabahi, M. Maalandish, R. S. Alishah, *High step-up DC-DC converter with reduced voltage stress on devices*, Int. Trans. Electr. Energ. Syst., 2018.
16. H. Mamur, R. Ahiska, *Application of a DC–DC boost converter with maximum power point tracking for low power thermoelectric generators*, Energy Convers. Manage, **97**, pp. 265–72(2015).